Supporting Information

Bioinspired multifunctional mechanoreception of soft-rigid hybrid actuator fingers

Shoulu Gong, Qifan Ding, Jiahao Wu, Wen-Bo Li, Xin-Yu Guo, Wen-Ming Zhang, Lei Shao**

S. Gong, Q. Ding, J. Wu, Prof. L. Shao

University of Michigan–Shanghai Jiao Tong University Joint Institute

Shanghai Jiao Tong University

Shanghai 200240, China

E-mail: lei.shao@sjtu.edu.cn

Dr. W.B. Li, X.Y. Guo, Prof. W.M. Zhang

School of Mechanical Engineering and State Key Laboratory of Mechanical Systems and Vibration

Shanghai Jiao Tong University

Shanghai 200240, China

Email: wenmingz@sjtu.edu.cn

Section I.The Schematic of human fingers

Mechanoreceptors are specialized neurons that transmit mechanical deformation information, as it can detect multiple stimuli, such as touch, virbation, contact, etc. As shown in **Figure S1**, the mechanoreceptors in fingers are the tactile corpuscles (a.k.a. Meissner corpuscles), located in the most developed tactile sensitive areas, such as the human fingers. In this paper, the fully printed force sensors are used to imitate the mechanoreceptors for the proposed HMAs.

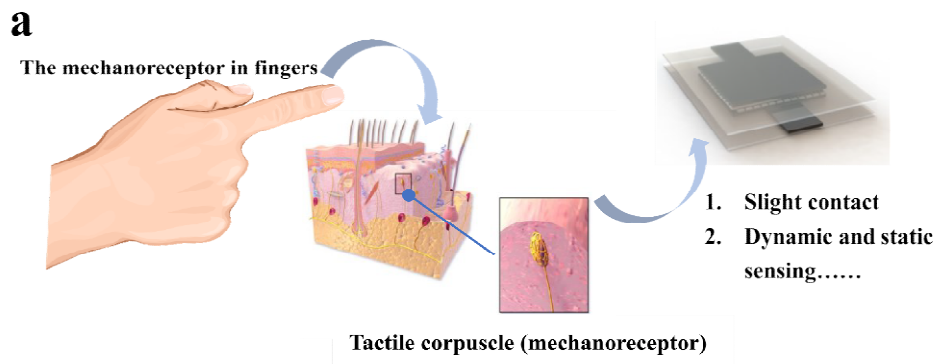

Figure S1. Schematics of human tactile sensations, and the flexible force sensors used for

HMAs acting as mechanoreceptors.

Section II.Assembly process of HMAs

Figure S2a shows the assembly process of the HMAs. The complete assembly process only costs serveral minutes and this soft-rigid hybrid actuator is about 116 mm in length and about 40 gram in weight. The hole in the Pedestal Frame is used to connect the air pump for actuation and thethreaded holes in the Pedestal Frame allow the HMAsto be easily installed on different gripper bases.

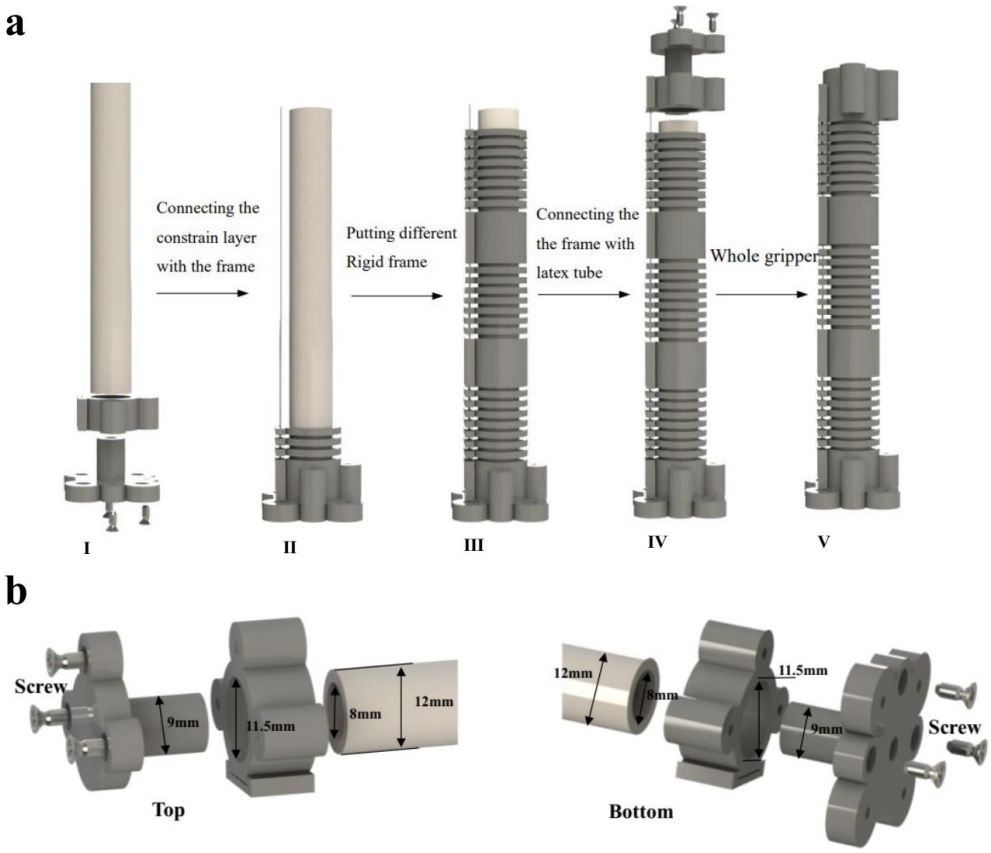

Figure S2. Assembling process of HMAs. (a) The complete assembling process includes five steps. First, we trim the soft tube to a proper length and then connect one end to a Pedestal Frame for sealing, with a Rigid Frame 3 outside the soft tube.Second, a constrain slab is fixed onto the Rigid Frame 3, which is used to restrict the installation direction of other Rigid Frames and constrain the bending direction of the HMA. Third, several sets of different Rigid Frames are mounted onto the soft tube in a fixed direction along the constrain slab in sequence (for example, 9 pieces of the Rigid Frame 1, 1 piece of the Rigid Frame 2, 9 pieces of the Rigid Frame 1, 1 piece of the Rigid Frame 2, 8 pieces of the Rigid Frame 1, and 1 piece of the Rigid Frame 3 are mounted in sequence). Fourth, a Top Frame is mounted to the other end of soft tube to seal it. Fifth,the HMA is completely assembled. (b) The schematic

diagramsshowing the used interference fitat the top and bottom of the HMA.

The interference fit is used to improve the air tightness of the HMAs. **Figure S2b** shows the connections between the Top Frame and the soft tube, and between the Pedestal Frame and the soft tube, respectively. The outer and inner diametersof the soft tube are 12 mm and 8 mm respectively, and therefore, one Pedestal Frame with an outer diameter of 9mm is used to form interference fit with the soft tube. Similarly, one Rigid Frame 3 with an inner diameter (11.5 mm) is used to form interference fit with the soft tube. Finally, we use self-tapping screws to fasten between the Rigid Frame 3 and the Pedestal Frame, and between the Rigid Frame 3 and the Top Frame, respectively.

Section III.Various bending behaviors of HMA

As shown in **Figure S3a(I)**, the Rigid frame2 will result in a discontinuous bending curve due to its length,which is similar as the discontinous bending of human fingers. Different bending behaviorsof HMAs can be achieved by changing the number, length and location of Rigid Frame 2. As shown in **Figure S3a(II)**, the HMA without Rigid Frame 2 bends continuously, while the HMA with a long Rigid Frame 2 (40 mm in length) at the bottom bends like a hook (**Figure S3a(III)** and **Figure S3b**).

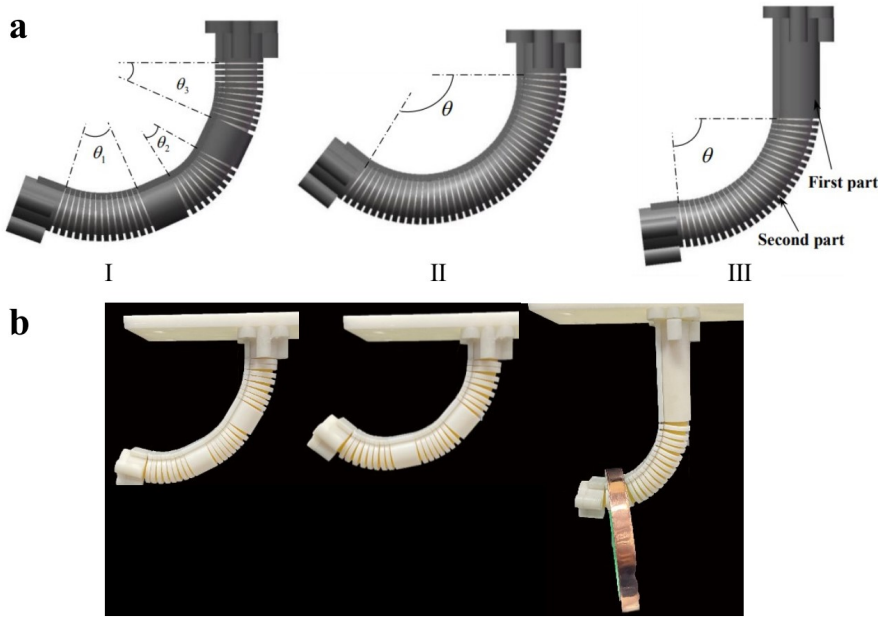

Figure S3. Different configurations of the rigid frames and resulted bending behaviors of HMAs. (a) Three different bendingmodes with two pieces of Rigid Frame 2, zero pieces ofRigid Frame 2 and one longer pieces ofRigid Frame 2. (b) Photographs of the bending modes correspondent to the simulation in **Figure S3a**.

Section IV.Kinematic model and actuation analysis of the HMAs

Here, we construct a kinematic model to analyze the deformation, motion and output force of the HMAs. Some reasonable assumptions are proposed for this kinematic model. First, an equivalent plate model is utilized to analyze the deformation of the elastic tube under different pressure, which means the geometric dimensions of the elastic tube is correspondent to the geometric dimensions of the plate (**Figure 4a**). Second, the rigid frames entirely restrict the radial expansion of the soft tube, and also the shorter frames (Rigid Frame 1) ensures continuous bending of the soft tube while the longer frames (Rigid Frame 2) results in a completely inflexible behavior when inflated (**Figure S4b**). Third, half of the soft tube is compressed while the other half is under tensile stress when the actuator bends (**Figure S4c**). Fourth, since the rigid frames only limit radial expansion, the outer shape of the soft tube is kept the same while only its inner shape deforms into an elliptical shape, leading to an offset of the centerline (undeformed neutral axis) of the soft tube from its original position.

Because the rigid frames are assumed to restrict radial expansion, the outer diameter of the soft tube is always kept at constant before and after pressure loading, and the plate width C is thus also a constant. Therefore, the stretching ratio along the width direction $\lambda_C = 1$, resulting in $\lambda_L \lambda_t = 1$. As shown in **Figure S4a**, when an air pressure is applied, a bending moment is caused by the force F, with the moment arm length l, which bends the actuator to an angle θ. This force F is caused by the loaded air pressure P. We thus obtain the following relationships

$$M_e = FB, \quad F = PS \tag{S1}$$

Figure S4bshows the effect of the Rigid Frame 2, which divides a continuous bending curve into two sections with angles θ_1 and θ_2. **Figure S4c**shows that half of the soft tube is under tensile stress while the other half is under compressive stress, divided along the neutral surface. Therefore, if the length of the centerline is L and $\Delta L = \theta D / 2$, then the length of tensile side becomes $L + \theta D / 2$, while the length of compressive side is $L - \theta D / 2$. The stretching ratios and thickness changes for these two halves can be calculated as:

$$\lambda_{L1} = \frac{L + \theta D/2}{L}, \quad \lambda_{t1} = \frac{1}{\lambda_{L1}} \tag{S2}$$

$$\lambda_{L2} = \frac{L - \theta D/2}{L}, \quad \lambda_{t2} = \frac{1}{\lambda_{L2}} \tag{S3}$$

$$\Delta t_1 = (1 - \lambda_{t1})t = (1 - \frac{L}{L + \theta D/2})t = \frac{\theta D}{2L + \theta D}t \tag{S4}$$

$$\Delta t_2 = (\lambda_{t2} - 1)t = (\frac{L}{L - \theta D/2} - 1)t = \frac{\theta D}{2L - \theta D}t \tag{S5}$$

Thickness changes at the top and bottom of the soft tube during the bending process, which leads to an approximately elliptical inner shape. This elliptical cross section results in a shift in the length of the moment arm. This offset in distance can be calculated as:

$$e = \frac{\Delta t_2 - \Delta t_1}{2} \tag{S6}$$

$$e = \frac{(\lambda_{t2} - 1)t - (1 - \lambda_{t1})t}{2} = \frac{2L\theta D}{(2L - \theta D)(2L + \theta D)}t \tag{S7}$$

The length of moment arm becomes $l' = l + e$.To ensure an accurate calculaiton of the shape of the inner cross section, the area correction ΔS is introduced to eliminate any errors in the above assumption of a perfect elliptical shape. The corrected inner cross-sectional area is $S' = \pi ab + \Delta S$, which can be calculated based on volume conservation of the soft tube. We assume the initial volume of the soft tube is V. After bending, this volume can be found by the following integral as:

$$V = \frac{1}{4}\pi(D^2 - d^2)L = \int_0^{(L+\theta D/2)} (\frac{1}{4}\pi D^2 - S')dL \tag{S8}$$

$$S' = \frac{d^2 L/4 + \pi D^3 \theta/8}{L + \theta D/2} \tag{S9}$$

$$\Delta S = -\pi ab + \frac{d^2 L/4 + \pi D^3 \theta/8}{L + \theta D/2} \tag{S10}$$

Thus, the bending moment can be calculated as$M_e = PS'l'$. The bending process of HMA can be regarded as a cantilever bimorph actuator whilethe constrain layer (shown in **Figure S4a**) will produce a resist moment M_c to maintain the fingertip at a fixed position, $M_c = M_e$, after reaching an equilibrium. The moment and blocking force of the constrain layer can be calculated by the well-known one-dimensional beam theory[41]:

$$M_c = \frac{bh^3 E\theta}{12L} = M_e = PS'l' \tag{S11}$$

$$F_b = \frac{3M_c}{2L} \tag{S12}$$

Based on this equilibrium, we can obtain the kinematic model about the relationship between pressure and bending angle for different constrain layer thicknesses, yielding:

$$\theta = \frac{12L(S'l')}{bh^3 E}P \tag{S13}$$

$$P = \frac{bh^3 E(L\theta + \theta^2 D/2)}{12Ll(d^2 L/4 + \pi D^3 \theta/8)} \tag{S14}$$

The moment of HMA euqals to the moment of constrain layer, and the output force (tip force) of HMA euqals the blocking force of the constrain layer at equilibrium. The tip force of HMA

(with different constrain layer thicknesses) under different pressure and bending angle can be also calculated based accordinlgy as:

$$F_{tip} = F_b \tag{S15}$$

$$F_{tip} = \frac{bh^3 E}{8L^2(Sl)}\theta S'l' \tag{S16}$$

$$F_{tip} = \frac{3PS'l'}{2L} = \frac{3P}{2L}\left(\frac{d^2 L/4 + \pi D^3\theta/8}{L + \theta D/2}\right)\bullet\left(l + \frac{2L\theta D}{(2L-\theta D)(2L+\theta D)}t\right) \tag{S17}$$

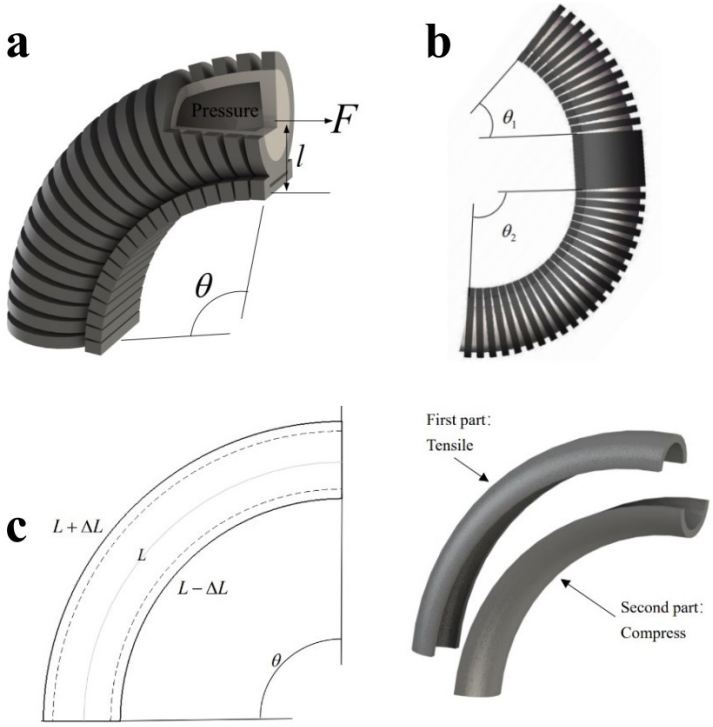

Figure S4. Actuation analysis of the HMA. (a) Deformation principle of the HMA. (b) The Rigid Frame2 divides the deformation into two sections. (c) Deformation of the soft tube during the bending process.

Section V.Principle of size estimation of grasped objects

Figure S5 shows the contact status between objects of different sizes and the HMA. As shown in **Figures5c**, the objects with a small size only contact the Force Sensor 1 during the whole grasping process. However, the objects with a large size will contact both Force Sensor1 and Force Sensor 2 during the grasping process shown in **Figure 5c**. The location of Force Sensor 1 imitates the distal phalanges of human fingers while the location of Force Sensor 2 imitates the intermediate phalanges. The number and location of sensorscan be adjusted to improve the resolution of objects size recognition.

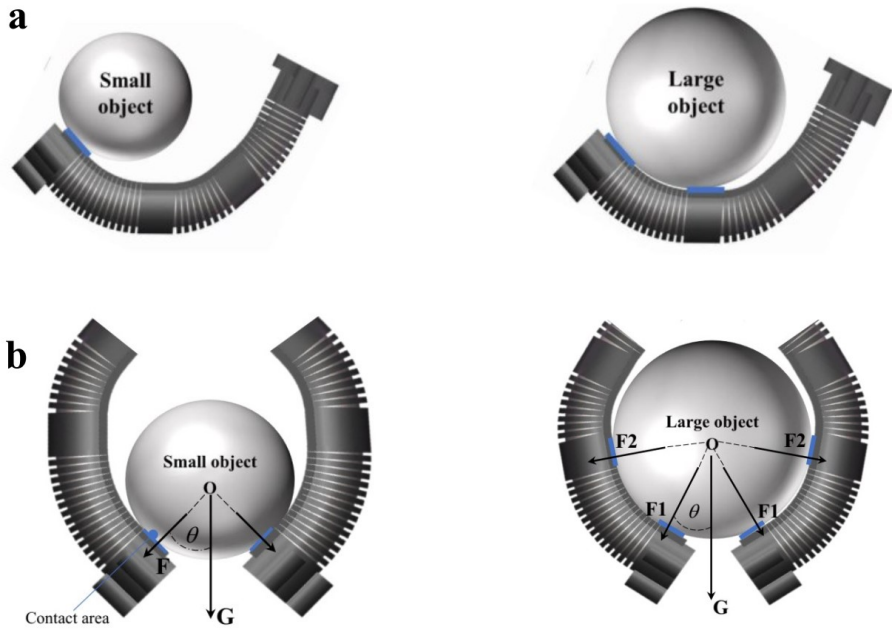

Figure S5. The contact status between HMAs and objects with different sizes. (a) Small objects only contact with the fingertip of the HMAs (Force Sensor 1), while large objects will contact with more locations with theHMAs (thus in contact with both ForceSensor 1 and Force Sensor 2inthis case). (b) Schematics of grasping of small and large objects.

Section VI.Contacting conditions of objects with different size and weight

As shown in **FiguresS6a –S6h**, these objects do not contact with Sensor 2 during the whole process due to their small sizes. Therefore, the output signal of Sensor 2 is almost constanly zero. The output signal of Sensor1 represents the grasping force, and this grasping force increases with the increase of the weight. On the other hand, as shown in **Figures S6i – S6k**, these objects are larger so they contact both Sensor 1 and Sensor 2 during the whole process.The grasping force is alsoclosely correlated with the weight of the objects.

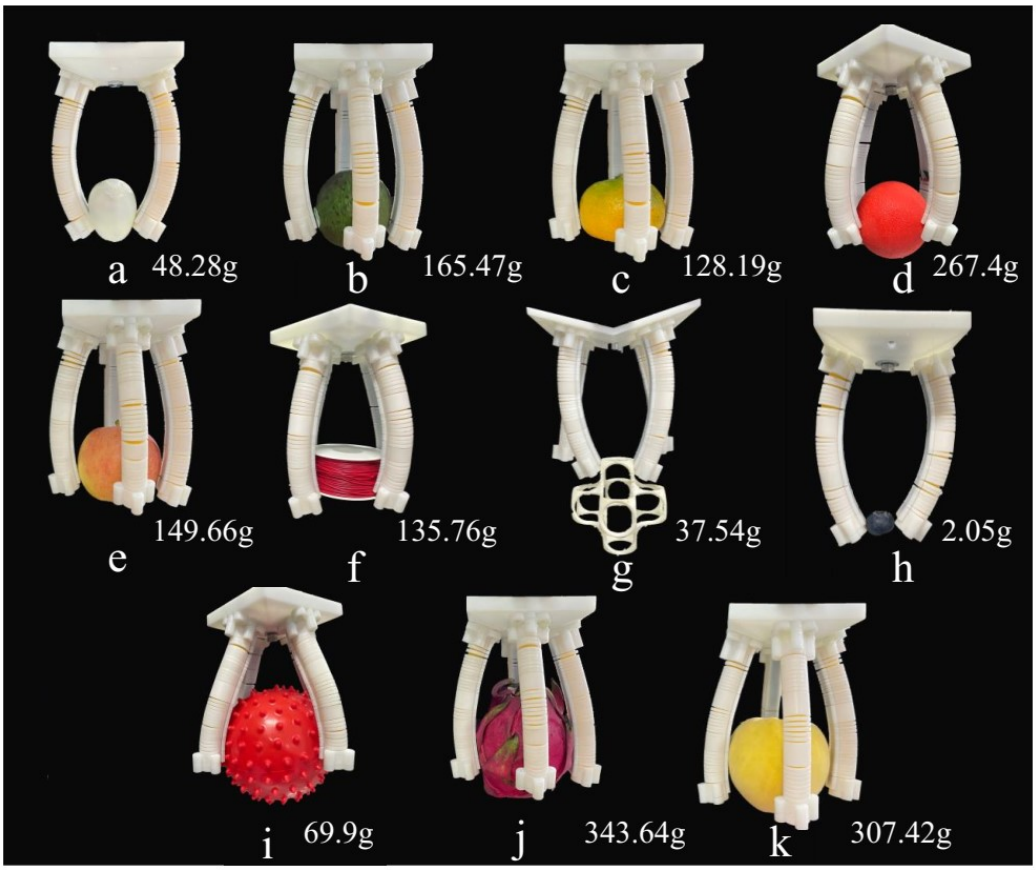

Figure S6. Contacting conditions of different objects. (a – h) Small objects of different weights only contact with the Sensor 1 at the tip of the HMA finger. (i – k) Large objects of different weights contact with both Sensor 1 (at the tip of the HMA finger) and Sensor 2 (at the middle of the HMA finger).